Shape Sensing a Morphed Wing with an Optical Fiber Bragg Grating

H. Tai

Langley Research Center, Hampton, Virginia 23681

Abstract: We suggest using distributed fiber Bragg sensors systems which were developed locally at Langley Research Center carefully placed on the wing surface to collect strain component information at each location. Then we used the fact that the rate change of slope in the definition of linear strain is very small and can be treated as a constant. Thereby the strain distribution information of a morphed surface can be reduced into a distribution of local slope information of a flat surface. In other words a morphed curve surface is replaced by the collection of individual flat surface of different slope. By assembling the height of individual flat surface, the morphed curved surface can be approximated. A more sophisticated graphic routine can be utilized to restore the curved morphed surface. With this information, the morphed wing can be further adjusted and controlled. A numerical demonstration is presented.

1. **Introduction**

It is well known that for different conditions of flight, a combination of different lifting surfaces is needed, such as wing, flap, and aileron. To further maximize efficiency, the idea of a morphed wing has been circulated for some time which covers a lot of technical areas, such as variable area, variable sweep, and/or variable shape (camber). In this short article, we limit our discussion to the last topics. Despite of the high interest, however only a limited number of articles have addressed this topics of shape sensing[1-4]. Before we can control the shape of the wing we have to possess the total information of the wing, especially the contour of the wing surface. In order to interrogate the condition of

a morphed wing we propose using distributed Bragg fiber sensors embedded on the wing surface to obtain the strain distribution on the wing. The distributed Bragg fiber sensor[5], developed locally by the Langley Research Center, has been proven to be ideal: light weight, small in size (typically 5 mm in length), immune to harsh environment, and easy to implement. The fiber sensor system is put on the wing when the wing is in a relaxed state, in which case, the sensor at each location registers zero strain. Once the wing is in a morphed (changed) state, each location will register a different strain reading. By processing the strain data the local curvature value is obtained. By assembling the values of local curvature for all locations, the contour shape of a morphed wing can be deduced.

2. **Theory**

The distributed optical fiber Bragg sensor system developed by the Langley Research Center has been proven very useful to measure strain for large aerospace structures. The sensors are embedded on the surface of the structure without harming its mechanical and aerodynamic performance, because of their light weight and immunity to electromagnetic disturbance. Fig.1, shows a section of wing projected onto the z-x plane, or the cross section of a wing at a certain span distance. The curves z_2 and z_1 are two surface curves representing the morphed state and natural state, respectively, say, of an upper surface of chord.

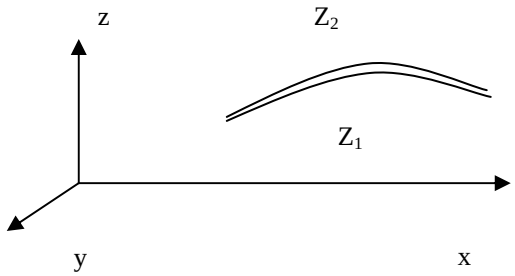

Fig. 1 A section of wing surface, z_1 represents the natural state; z_2 represents the morphed state

The surface of a wing in a morphed state can be represented by the totality of all points of

z_2

$$z_2 = z_2(x, y)$$
$$with \;\; x_l \le x \le x_u \;\; and \;\; y_l \le y \le y_u$$

as the boundaries of a wing or specifically a special section of the wing. While in its natural state (or un-morphed state), we have $z_1 = z_1(x, y)$. If the sensor system was placed on the surface while the surface in its natural state, then the sensor system shows zero strain at every location. While the surface is its morphed state, it is stretched or compressed, either due to bending or other artificial means, such as forcing at certain places by mechanical means. The optical sensor will register a non-zero strain reading corresponding to the stressed state at each location. Since current state-of-the- art optical fiber Bragg sensors only can measure the strain in one dimension, we have to carefully lay the fiber sensor either parallel to x or y direction. In other words, we measure the x component strain and y component strain simultaneously. Suppose we measure the x direction strain at a certain location, we have[6]

$$\frac{\int_{x_1}^{x_2}\sqrt{1+(\frac{\partial z_2}{\partial x})^2}\,dx-\int_{x_1}^{x_2}\sqrt{1+(\frac{\partial z_1}{\partial x})^2}\,dx}{\int_{x_1}^{x_2}\sqrt{1+(\frac{\partial z_1}{\partial x})^2}\,dx}=\varepsilon_x \qquad (1)$$

Where, we have the basic definition of linear strain in x direction as ε_x expressed as the difference of the arc length in the morphed state and natural state. Where x_1 and x_2 are the limits of the linear sensors. ε_x can be determined accurately using our optical Bragg sensor if the strain value is small or the strain is uniform. However, when the strain value is large and non-uniform (say, on the order of 10^{-2}) the optical Bragg sensor sometimes gives a non-unique value and has to be determined judiciously[7].

Equation (1) is exact, however if we approximate Eq. (1) by assuming the variation of the partial derivative is minute within the limits x_1, and x_2, so the integrand assuming an average value can be taken out of the integration. This is our first approximation. We have

$$\sqrt{1+(\frac{\partial z_2}{\partial x})^2}=(1+\varepsilon_x)\sqrt{1+(\frac{\partial z_1}{\partial x})^2}$$

or

$$1+(\frac{\partial z_2}{\partial x})^2=(1+\varepsilon_x)^2[1+(\frac{\partial z_1}{\partial x})^2] \qquad (2)$$

or

$$\frac{\partial z_2}{\partial x}=\sqrt{(1+\varepsilon_x)^2[1+(\frac{\partial z_1}{\partial x})^2]-1}$$

$\frac{\partial z_1}{\partial x}$ is known ahead of time and ε_x is the measured value. Therefore $\frac{\partial z_2}{\partial x}$ value is obtained.

By the same token, $\frac{\partial z_2}{\partial y}$ value is obtained.

We noticed that by taking this linearization process, we have successfully inverted the problem. Namely, the surface linear slope can be expressed in term of the local strain as shown as in Eq. (2)

We carefully lay the sensors at the location, $x_i, i = 1, i_{\max}, y_j, j = 1, j_{\max}$,so $\varepsilon_x^{i,j}$ values are

measured. Then the partial derivatives $\frac{\partial z_2^{i,j}}{\partial x}$ *and* $\frac{\partial z_2^{i,j}}{\partial y}$ are obtained. Let's reproduce Eqs. (2) where the index *i, j* refer the station location.

$$\frac{\partial z_2^{i,j}}{\partial x} = \pm\sqrt{(1+\varepsilon_x^{i,j})^2[1+(\frac{\partial z_1^{i,j}}{\partial x})^2]-1} \equiv c_1$$
$$\frac{\partial z_2^{i,j}}{\partial y} = \pm\sqrt{(1+\varepsilon_y^{i,j})^2[1+(\frac{\partial z_1^{i,j}}{\partial y})^2]-1} \equiv c_2 \qquad (3)$$

Eq.(3) has a simple solution, i.e., an equation of linear plane

$$z_2 = c_1 x + c_2 y + c_3 \qquad (4)$$

Where the superscript index *i,j* have been removed; c_1, and c_2, are constants defined by Eq. (3). c_3 is a constant referred as the vertical height at that particular location, but we have no accurate information to obtain this value. Since the equation (3) involves the square root of strain value, care has to be taken that when the strain is negative corresponding to compression, the c_1, c_2 values are taken as negative pure real numbers. Originally, the plane is limited to the domain covered by sensors, however, since it is a plane, it can be extended. A natural extension could be chosen as the mid-point between

the next sensor location and boundary of the plane. The layout is shown in Fig.2. Eq.(4) tells us the contour of the wing is reconstructed by a series of rectangular planes, (or rectangular tiles) i.e., the

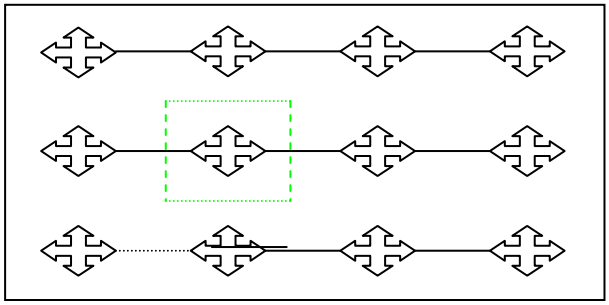

Fig. 2, Sensor layout diagram. The area enclosed by the dashed borders forms a plane determined by the strain. The sensor is indicated by the arrows.

derivatives are not continuous between the plane boundaries. If we carefully place the sensors at the intersection of grid points, say, at equal distance (nevertheless, that is not necessary) then around that point, a square of plane is formed which gives two important data, i.e., the slope of square plane along x and y direction, c_1 and c_2. In order to reconstruct the contour of the wing, we still need the value of c_3, which can be approximated by $z_1^{i,j}$ which is the height of location in the natural state. This is another assumption in our approximation. What we are saying is that the change of strain is primarily and uniquely due to the change of the average slope of the arc. With all the information, we can reconstruct the whole contour of the wing in the morphed state.

4. Deficiency of the Model

What we have done is to replace the strain by the average slope of the area covered by the sensor. Then, we ask the question what happens if the sensor is on top of a surface which is absolutely horizontal and nevertheless, the strain is not zero. Another question is based

on Eq.(3), given the strain value, we can not tell if the slope is positive or negative. However, if we place three sensors in a row and if the first one registered positive slope and the third one registered negative slope, then we can infer that somewhere in between them the surface is completely flat. Fortunately for the morphed wing case, the deformation is well kept in a fixed range and a lot of experiments and testing are needed to resolve the ambiguities.

5. Numerical Model

To demonstrate numerically how the measured strain values generate the morphed contour surface, we build a panel of dimension 6 x 5 which has 30 unit cells. Rather placed the sensor in the middle of cell, we place at the corner of the cell. At each corner, the optical distributed sensors were embedded which simultaneously and independently measured the x and y component of strain. To make everything simpler, we chose the un-morphed surface as a flat surface, so from Eq. (3)

$$c_1 \square \sqrt{2\varepsilon_x}$$
$$c_2 \square \sqrt{2\varepsilon_y} \qquad (5)$$

If we decide to poke the panel at the location of the center of cell C_{32}, i.e., the cell in column 3 and row 2. Accordingly, the nearby sensors would register a much higher values than the sensors far away. The following mocked up sensor values distribution are adopted to demonstrate the idea.

Table 1 Strain Values

X component

0.0001	0.0001	0.0001	0.0002	0.0001	0.0001
0.0001	0.001	0.002	0.0015	0.001	0.0001
0.0001	0.0005	0.0017	0.0014	0.0012	0.00014
0.0001	0.0005	0.001	0.001	0.0005	0.00014
0.0001	0.0001	0.0001	0	0	0

Y component

0.0001	0.0001	0.0001	0.0002	0.0001	0.0001
0.0001	0.001	0.002	0.0015	0.001	0.0001
0.0001	0.0005	0.0017	0.0014	0.0012	0.00014
0.0001	0.0005	0.001	0.001	0.0005	0.00014
0.0001	0.0001	0.0001	0	0	0

With this strain distribution, we generate the contour surface shown below.

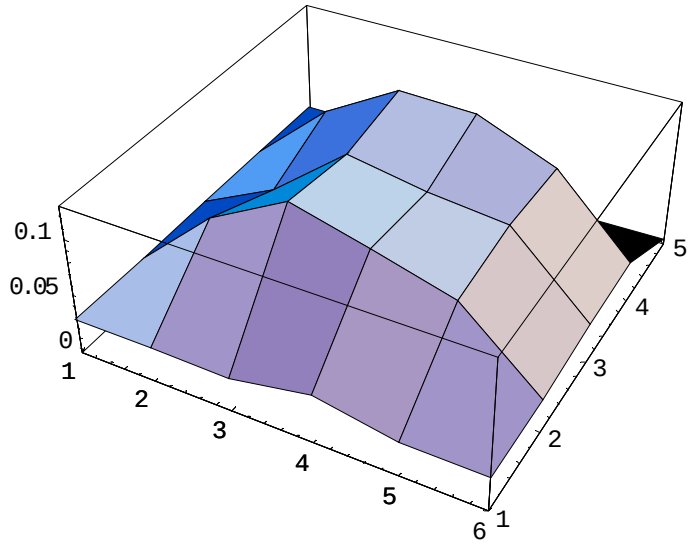

Fig.2 surface contour

6. Conclusion

This is the first attempt to analyze and control a morphed wing using distributed optical Bragg sensors to measure the local strain due to the deformation of wing surface. Based on the measured strain values, we have used a physical (and drastic) approximation to recreate the morphed contour, not as a continuous surface, but as a zigzag first order flat surface. With the help of graphic software we can make a smooth, continuous contour

surface. We believe this approach to be not only feasible but also practical. Because the distributed optical Bragg sensor system is light weight, it is quite easy to implement hundreds or thousands of sensors embedded on the wing. However, we have to pay attention to the following aspects.

(a) The readout and information process almost are instantaneous and accurate, provided the whole operation is carried out in a laboratory setting. However, when the system is airborne, subjected to dynamic vibration, it may impose some difficulties in the laser response and readout system. A reliable, steady, and robust laser readout system is highly desirable.

(b) We further point out that the morphed state also depends on other variables which may be minor, such as temperature and pressure, therefore careful calibration is important.

(c) Careful and strategic planning is needed for the choice of embedded sensor location. We suggest placing the sensors in the areas of aerodynamically sensitive areas, such as the leading edge and quarter chord areas.

(d) Based on this algorithm, a morphed wing is replaced by a collection of zigzag surface of rectangular tiles. However, smoothing graphic software can be used to show the morphed wing as a continuous surface. We emphasize that it is not important that the reconstructed morphed surface looks exactly the same as the real one as long as the real surface can be inferred from the information of the reconstructed surface.

(e) Many laboratory and ground tests will be needed to verify this technique, so that a one to one correspondence between strain distribution and the contour information of the wing is firmly established.

This is a simple and crude model, but we believe this technology can give us reliable information about a morphed wing. Many tests will have to be conducted, and of course the use of right software will be necessary to give a graphic representation. With this technique, we have established a one to one relationship between strain state and morphed state of a wing.

6.References

1. P. B. Bogert, E. Haugse, and R. E. Gehrki, " Structure shape identification from experimental strains using a modal transformation technique", 44th AIAA/ASME/ASCE/AHS Structures, Structureal Dynamics, and Materials Conference, 7-10 April 2003, Norfolk, VA

2. S. Shkarayev, R. Krashantisa, and A. Tessler, " An Inverse Interplolating Method Utilizing in-Flight Strain Measurements for determining oads and Structural Response of Aerospace Vehicles," Proceeding of the Third Intenational Workshop on Structural Health Monitoring, Stanford, CA 2001, pp. 336-343.

3. S. Shkarayev, A. Raman and A. Tessler, "Computational and Experimental Validation Enabling a Viable in-Flight Structural Health Monitoring Technology," Proceeding of the Third Intenational Workshop on Structural Health Monitoring, Cachan (Paris), France 2002, pp. 1145-1150.

4. A. Tessler and J. L. Spangler, " Inverse FEM for full-field Reconstruction of Elastic Deformations in Shear Deformable Plate and Shells", 2nd European Workshop on Structural Health Monitoring, July 7-9, 2004, Munich, Germany.

5. M. Froggatt, "Distributed measurement of the complex modulation of a photo-induced Bragg grating in an optical fiber", Applied Optics, v. 35, no 25, 1996.

6. G. B. Thomas, Jr and R. L. Finney, "Calculus and Analytic Geometry", Addison and Wesley Publishing Company, 1979

7. H. Tai, "Simple numerical simulation of strain measurement", SPIE's 47 Annual meeting, July 5-11, 2002.